In Vivo Detection of ParaCEST Contrast Agents at 9.4T

Nevin McVicar[1], Alex Li[2], Mojmir Suchy[2,3], Robert H Hudson[3], and Robert Bartha[1,2]

[1]*Medical Biophysics, University of Western Ontario, London, ON, Canada,* [2]*Imaging Research Group, Robarts Research Insitute, London, ON, Canada,* [3]*Chemistry, University of Western Ontario, London, ON, Canada*

Target audience: Physicists and chemists developing paramagnetic magnetic resonance imaging (MRI) contrast agents that produce contrast via chemical exchange saturation transfer (paraCEST), especially those scientists developing agents with *in vivo* applications.

Purpose: ParaCEST MRI contrast agents have reduced *in vivo* sensitivity due to magnetization transfer effects from endogenous macromolecules. The purpose of this study is to compare the *in vivo* sensitivity of four different paraCEST agents and evaluate whether *in vivo* performance can be predicted from *in vitro* characterization of the MR properties of each agent.

Methods: The synthesis methods of (Dy^{3+},Tb^{3+},Tm^{3+})-DOTAM-Gly-Lys and Eu^{3+}-DOTAM-Gly-Phe have been previously described[1]. ***In vitro:*** Aqueous pH 7.0 phantoms containing 10mM paraCEST agent were prepared to study agent properties using a 9.4 T horizontal bore Agilent MRI scanner equipped with a 3 cm millipede RF volume coil (Agilent, Palo Alto, CA). Using omega plots as described by Sherry et. al., exchange rates of the amide and/or bound protons were measured at 37 ^{o}C using a 5s saturation pulse with different saturation powers (B_1 = 8, 10, 12, 14, 16 μT)[2]. T_1 relaxation time constants were measured using a standard inversion recovery experiment. *In vitro* CEST experiments were performed using a fast spin echo (FSE) pulse sequence. ***In vivo:*** All *in vivo* MRI experiments were acquired on the same 9.4 T MRI scanner equipped with a custom-built 3 cm diameter RF surface coil. *In vivo* studies were performed using three healthy mice per agent. Anaesthetized mice were secured on an MRI-compatible stage to restrict leg motion. Pre-injection high-resolution T_2-weighted anatomical images were acquired using a fast imaging with steady state precession (FISP) pulse sequence. CEST spectra were acquired from the same slice pre- and post-injection. A fast spin echo (FSE) pulse sequence was used for CEST imaging preceded by a continuous wave presaturation pulse (B_1 = 14 μT, TS = 5s). Saturation pulse frequencies used to acquire CEST spectra included ±1*(1000, 20, 10, 5, 3, 2, 1 ppm) and 0 ppm along with 31 frequencies (Δ=1ppm) centered on the expected chemical shift based on *in vitro* results. Following pre-injection anatomical image and CEST spectra acquisition, 25 μL of 100 mM paraCEST agent dissolved PBS was injected directly into a leg muscle. Post-injection CEST spectra acquisition began within 15 minutes of injection. Animal procedures were performed according to a protocol approved by the Western University Animal Use Subcommittee.

Table 1

Agent	Lifetime (μsec)	T_1 (s)	CS (ppm)	*In vitro* CEST (%)	*In vivo* CEST (%)
Tm^{3+}-DOTAM-Gly-Lys-OH	926	0.910	-46	22	2.6
Tb^{3+}-DOTAM-Gly-Lys-OH	273	1.838	59	14	5.4
Dy^{3+}-DOTAM-Gly-Lys-OH	919	0.563	73	11	2.5
Eu^{3+}-DOTAM-Gly-Phe-OH	613	2.988	44	24	7.5

Results: Table 1 shows the bound lifetimes of the amide (Dy^{3+},Tb^{3+},Tm^{3+}) and bound (Eu^{3+}) protons, T_1 relaxation time constants along with the chemical shift (CS) and paraCEST contrast achieved both *in vitro* and *in vivo*. Figures 1A and 1B demonstrate representative results for one mouse experiment for Eu-DOTAM-Gly-Phe. Figure 1A provides an average pre-injection paraCEST spectrum along with the corresponding average post-injection CEST spectra superimposed on top. Average pre-injection paraCEST spectra are generated using only the pixels that achieved paraCEST contrast in post-injection CEST spectra. Figure 2A demonstrates a post-injection paraCEST contrast map. Only pixels' achieving contrast to noise ratio (CNR)$\geq 2\sqrt{2}$ (ie. probability of real CEST contrast = 95%) were used to generate the in vivo CEST maps[3].

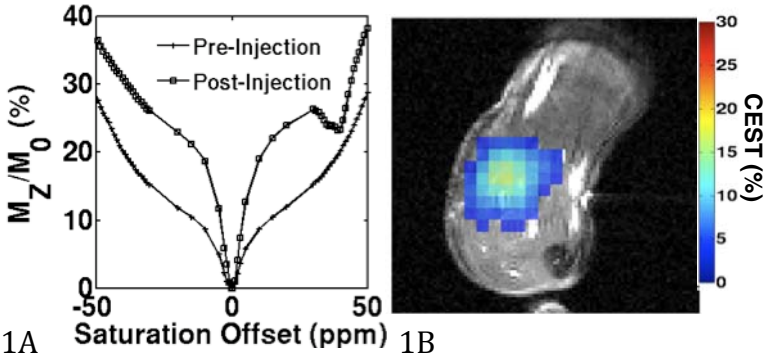

1A 1B

Discussion: *In vitro* agent parameters (Table 1) vary significantly between agents. Based on Table 1, a short T_1 relaxation time *in vitro* suggests limited *in vivo* CEST contrast generation (Dy^{3+}, Tm^{3+}). Eu^{3+} and Tb^{3+} agents both have relatively long bound lifetimes (~1ms) along with long (>1s) T_1 relaxation times and therefore it is reasonable that both agents achieved significant CEST contrast both *in vitro* and *in vivo*. Interestingly, all agents appeared to clear from the injection site within 60 minutes. Significant changes in the endogenous MT effects were observed following paraCEST injection. These changes appear to be caused by either a decrease in local T_1, and/or an increase in local water content.

Conclusion: Four different paraCEST agents were detected *in vivo* using CEST contrast. This finding represents a significant step forward for paraCEST contrast agents. *In vitro* agent performance appears to provide significant insight into the agents *in vivo* capabilities. The saturation pulse was identical for each paraCEST agent and thus agent-specific optimization should generate greater CEST contrast *in vivo*.

References: 1. Wojciechowski et al. *Bioconjug Chem.* 18(2007): 1625-1636 2. Dixon et al. *Magnetic Resonance in Medicine* 63(2010): 625-632. 3. Haacke, E.M. et al. *John Wiley & Sons, Inc.* (1999).